ACS APPLIED MATERIALS & INTERFACES

Research Article

www.acsami.org

Highly Selective Detection of Polycyclic Aromatic Hydrocarbons Using Multifunctional Magnetic–Luminescent Molecularly Imprinted Polymers

Hao Li and Leyu Wang*

State Key Laboratory of Chemical Resource Engineering, School of Science, Beijing University of Chemical Technology, Beijing 100029, China

Supporting Information

ABSTRACT: A facile method is presented for the selective luminescence detection of trace polycyclic aromatic hydrocarbons (PAHs) based on a combination of the specific recognition of molecularly imprinted polymers (MIPs) and magnetic separation (MS). Multifunctional magnetic–luminescent MIP nanocomposites were fabricated via a one-pot emulsion strategy using polystyrene-co-methacrylic acid copolymer, hydrophobic Fe_3O_4 nanoparticles and luminescent $LaVO_4$:Eu^{3+} nanoparticles as building blocks with a phenanthrene template. The resulting nanocomposites can be employed in a simple method for the luminescence detection of phenanthrene. Furthermore, magnetic separation of the nanocomposites from the target mixture prior to luminescence detection of phenanthrene affords significantly enhanced selectivity and sensitivity, with a 3σ limit of detection (LOD) as low as 3.64 ng/mL. Milk samples spiked with phenanthrene (5.0 μg/mL) were assayed via this method and recoveries ranging from 97.11 to 101.9% were obtained, showing that our strategy is potentially applicable for the preconcentration, recovering, and monitoring of trace PAHs in complex mixtures.

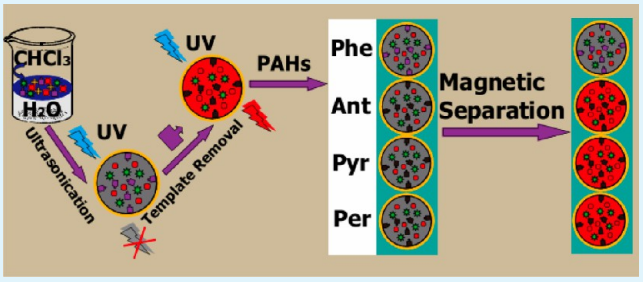

KEYWORDS: *magnetic separation, molecularly imprinted polymers, luminescence detection, polycyclic aromatic hydrocarbons (PAHs), nanocomposites, selectivity*

INTRODUCTION

Polycyclic aromatic hydrocarbons (PAHs) are a class of persistent organic pollutants (POPs) that are ubiquitous in the environment—including air, water, and soil. Major sources of POP contamination include the incomplete combustion of coal and gasoline and the use of tobacco products, as well as natural sources such as vegetation fires and volcanic eruptions. As PAHs and their analogues are strongly potent carcinogens and mutagens and may be transferred from plants to dairy food and finally to animals and humans, they have been studied with great interest for decades.[1−7] A variety of methods such as high-performance liquid chromatography (HPLC),[8−10] gas chromatography (GC),[11] gas chromatography–mass spectrometry (GC-MS),[12,13] capillary electrophoresis,[14] surface-enhanced Raman scattering (SERS),[15,16] and matrix-assisted laser desorption ionization-time of flight mass spectrometry (MALDI-TOF-MS)[17] have been developed for the detection of PAHs. However these techniques involve laborious pretreatment of samples containing traces of PAHs and are expensive and time-consuming. In addition, the similar structures of PAHs inhibit their selective quantification. Thus, developing a simple, sensitive, and highly selective method for detection of trace PAHs still remains a challenge.

Molecularly imprinted polymers (MIPs) have been widely used as artificial antibodies in biochemical analysis because of their distinct advantages over their biological counterparts, such as inherent mechanical/chemical stability,[18,19] high selectivity to target molecules,[20,21] low cost,[22] short development time,[23] and ease of preparation.[24] Generally, the in situ polymerization of functional monomers and cross linkers is employed in the synthesis of MIPs and the target templates are encapsulated in the polymer matrixes via hydrogen bonds or covalent interactions between templates and monomers.[25−27] However, PAHs usually have no active functional groups and only can be dispersed in organic solvents, and thus the in situ polymerization method is not suitable for the preparation of MIPs for PAH detection.[28]

Luminescent nanoparticles (NPs) incorporated in MIPs have shown great potential as sensors for a wide range of applications.[29−31] However, due to the similar UV-absorption spectra of PAHs, luminescence quenching by other PAHs (and other aromatic species) results in low selectivity when luminescent MIPs are employed as a sensor for a specific

Received: May 29, 2013
Accepted: October 2, 2013
Published: October 2, 2013

PAH in solution. Our previous work has demonstrated that the advantages of MIPs and luminescent nanoparticles can be combined for the detection of organophosphate pesticides.[32,33] Furthermore, we have previously encapsulated magnetic NPs in magnetic−luminescent nanocomposites, although the magnetic properties were used only for the collection of nanocomposites during the synthesis process rather than to enhance the detection selectivity.[33] In this work, we extend our previous efforts to the fabrication of trifunctional magnetic−luminescent MIP nanocomposites using a facile encapsulation strategy, and show how magnetic separation of the nanocomposites from the target mixture prior to luminescence detection of PAHs affords significantly enhanced selectivity.

As shown in Scheme 1, with the help of ultrasonication, the hydrophobic luminescent NPs, magnetic NPs, and template molecules (phenanthrene) were encapsulated in an amphiphilic polymer matrix. After the removal of phenanthrene by elution followed by magnetic separation, the MIP nanocomposites were obtained. On addition of phenanthrene (Phe), anthracene (Ant), pyrene (Pyr), or perylene (Per), the luminescence of the MIP nanocomposites was quenched dramatically. After magnetic separation of the nanocomposite from the mixture, the red luminescence was recovered in the cases of anthracene, pyrene, and perylene. Whereas in the case of phenanthrene, the luminescence was still quenched and no recovery was observed. These results highlight the good selectivity that can be obtained by incorporating a magnetic separation step in the luminescence detection of phenanthrene in the presence of other PAHs. This is the first report to dramatically enhance the selectivity of PAH detection via magnetic separation based on the luminescent−magnetic MIPs nanocomposites.

Scheme 1. Fabrication of Multifunctional Molecularly Imprinted Polymer (MIP) Nanocomposites and the Selective Luminescence Detection of Phenanthrene in the Presence of Anthracene, Pyrene, and Perylene by Means of Magnetic Separation

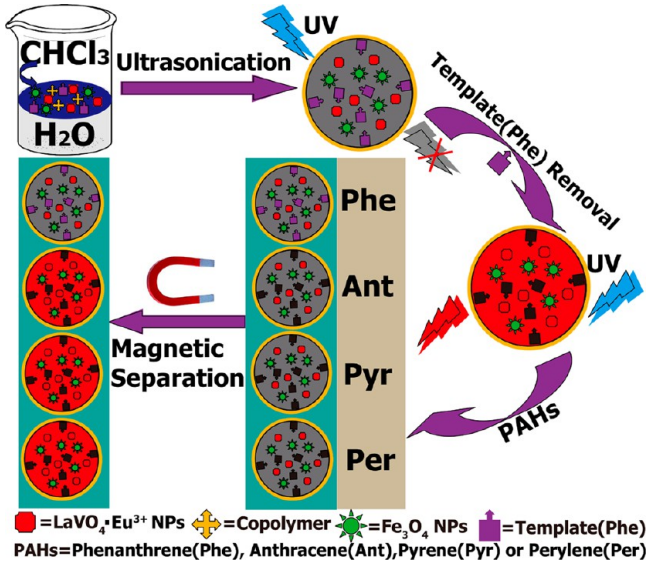

EXPERIMENTAL SECTION

Reagents. $La(NO_3)_3{\cdot}6H_2O$ and $Eu(NO_3)_3{\cdot}6H_2O$ (purity>99.9%) were purchased from Beijing Ouhe Chemical Reagent Company. Oleic acid, ethanol, cyclohexane, chloroform, NaOH, acetone, methanol, and *N*,*N*-dimethylformamide (DMF) were obtained from Beijing Chemical Factory. $Fe(NH_4)_2{\cdot}(SO_4)_2{\cdot}6H_2O$, styrene (St), methacrylic acid (MAA), 2,2′-azobisisobutyronitrile (AIBN), and NH_4VO_3 were purchased from Tianjin Fuchen Chemicals Co. The styrene was purified before use. The polycyclic aromatic hydrocarbons (PAHs) anthracene (Ant), phenanthrene (Phe), pyrene (Pyr), and perylene (Per) used in this work were obtained from Aladdin (Shanghai).

Instrumentation. A UNICO 2802PC spectrophotometer was used to obtain absorption spectra. The morphology characterization of the nanocomposites was carried out on a Hitachi H-800 transmission electron microscope (TEM). A Rigaku XRD-A112 X-ray diffractometer was used to record the X-ray diffraction (XRD) patterns. The emission spectra were measured using a Hitachi F−4600 fluorescence spectrophotometer equipped with a plotter unit and a quartz cell (1 cm × 1 cm).

Synthesis of Magnetic Fe_3O_4 Nanoparticles (NPs). The Fe_3O_4 NPs were synthesized according to a previously reported strategy with some modifications.[34] Briefly, NaOH (1.0 g), deionized water (5.0 mL), and oleic acid (9 mL) were added to ethanol (15 mL) under magnetic stirring. A solution of $Fe(NH_4)_2(SO_4)_2{\cdot}6H_2O$ (0.784 g) in water (8 mL) was then added and the solution was thoroughly stirred before the solution was transferred into a 45 mL Teflon-lined autoclave and heated at 180 °C for 11 h. After the reaction system was cooled to room temperature, the resulting black powder was washed with chloroform and ethanol and collected. The product was then dispersed in chloroform (1.0 mL) and stored for later use.

Preparation of Luminescent $LaVO_4$:Eu^{3+} NPs. The red luminescent $LaVO_4$:Eu^{3+} NPs were prepared via a modified one-pot solvothermal method.[35] Briefly, NH_4VO_3 (0.06 g), NaOH (0.6 g), deionized water (5 mL), and ethanol (22 mL) were added into an autoclave under stirring before the addition of oleic acid (10 mL). An aqueous solution of $La(NO_3)_3{\cdot}6H_2O$ (980 μL, 1.0 mol/L) and $Eu(NO_3)_3{\cdot}6H_2O$ (20 μL, 1.0 mol/L) was added and stirring was continued for 15 min. Then, the autoclave was heated for 6 h at 140 °C. The resulting solid was washed twice with ethanol and cyclohexane. The product was then dispersed in 1.0 mL of chloroform.

Fabrication of Polystyrene-co-methacrylic Acid (poly(St-co-MAA) Copolymer. The poly(St-co-MAA) copolymer was synthesized in accordance with the previously reported methods.[31,33,36] Briefly, 0.2 g of MAA, 4.6 g of styrene (St/MAA = 95:5 mol %), 0.096 g of AIBN, and 35 mL of chloroform were added into an autoclave under magnetic stirring. The autoclave was then heated at 100 °C for 10 h. The copolymer was purified by washing twice with 80 mL of methanol. To record its XRD pattern, the white powder was dried at 70 °C for 10 h.

Preparation of MIP Nanocomposites. The MIP nanocomposites were synthesized using an ultrasonication encapsulation method. Briefly, phenanthrene (Phe) (10 mg), $LaVO_4$:Eu^{3+} NPs (10 mg), Fe_3O_4 NPs (10 mg), and St-co-MAA copolymer (30 mg) were mixed together and diluted to 1.0 mL by adding chloroform. The resulting solution was injected into 10 mL of sodium hydroxide solution (70 μg/mL) and then stirred at 60 °C for 2 h with ultrasonication. The as-prepared MIP nanocomposites were washed twice with acetone (5 mL) to remove the imprinted templates (phenanthrene). Finally, the functional MIP nanocomposites were dispersed into ethanol with a final concentration of 8 mg/mL and stored for later use. Nonimprinted polymer (NIP) nanospheres were prepared via the same protocol in the absence of phenanthrene template molecules.

Incubation Time Tests. MIP nanocomposites (200 μg) were exposed to 1 mL of phenanthrene solution in ethanol (5 μg/mL) and incubated at 25 °C. The degree of luminescence quenching was monitored from 0 to 900 min with a time interval of 30 min.

Phenanthrene Detection. Standard solutions of anthracene, phenanthrene, pyrene, and perylene were obtained by dissolution in DMF, ethanol, ethanol, and chloroform, respectively. The MIP nanocomposite (200 μg) obtained using phenanthrene as the template was mixed with different amounts of PAHs and the mixture diluted to 1 mL with ethanol. The samples were incubated for 90 min at 25 °C and then separated using a magnet before the luminescence measurements were carried out.

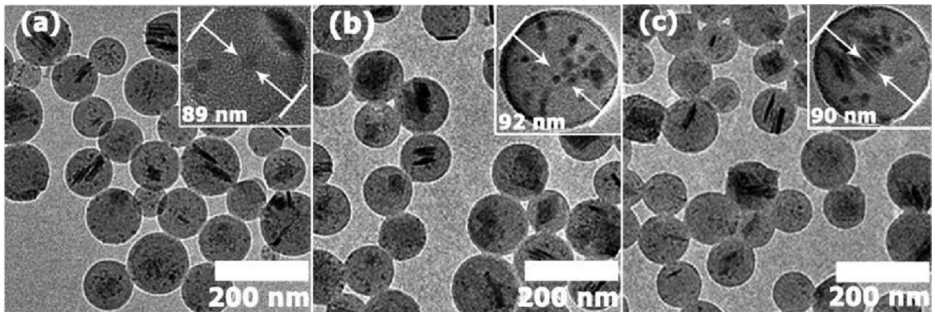

Figure 1. Transmission electron microscopy images of (a) NIP and MIP nanocomposites (b) before and (c) after the removal of the template by elution.

Adsorption Isotherm Tests. The MIPs (8 mg) or NIPs (9 mg) were suspended in 2.0 mL of ethanol with the addition of varying amounts (0.1−0.6 mg/mL) of phenanthrene. The samples were incubated at 25 °C for 90 min. The supernatant was obtained by magnetic separation and monitored by UV−vis spectrophotometry, and the isotherm plots were then constructed. All the binding experiments were carried out in triplicate.

RESULTS AND DISCUSSION

The MIP nanocomposites were fabricated by encapsulating magnetic Fe_3O_4 NPs, luminescent $LaVO_4:Eu^{3+}$ NPs, and phenanthrene in polymer matrixes using a facile ultrasonication emulsion strategy. The shape and size of the as-prepared MIP nanocomposite particles were monitored by transmission electron microscopy (TEM). The images of NIPs (Figure 1a) and MIPs before (Figure 1b) and after (Figure 1c) the removal of templates show that the average size of the nanocomposite particles was approximately 90 nm in each case, and no significant differences can be observed. Large magnification TEM images reveal that both the $LaVO_4:Eu^{3+}$ and Fe_3O_4 NPs are well-distributed in the polymer matrixes. The presence of both $LaVO_4:Eu^{3+}$ and Fe_3O_4 NPs was confirmed by powder X-ray diffraction (XRD) (Figure 2). The peak positions and

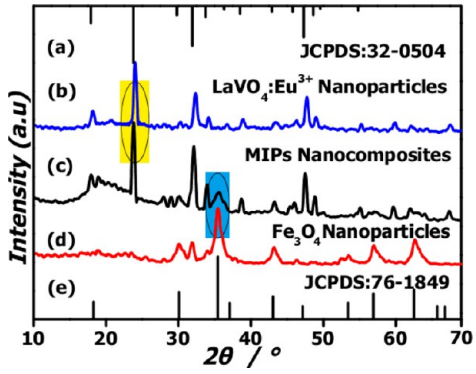

Figure 2. XRD patterns of (a) standard $LaVO_4:Eu^{3+}$ (JCPDS card 32-0504), (b) $LaVO_4:Eu^{3+}$ NPs, (c) MIP nanocomposites, (d) Fe_3O_4 NPs, and (e) standard Fe_3O_4 (JCPDS card 76-1849).

relative intensities in the patterns of $LaVO_4:Eu^{3+}$ NPs (Figure 2b) and Fe_3O_4 NPs (Figure 2d) agree well with the data reported in the JCPDS standard card (No. 32-0504, Figure 2a) and JCPDS standard card (No. 76-1849, Figure 2e), respectively. The XRD pattern of the MIP nanocomposites (Figure 2c) confirms that both the luminescent $LaVO_4:Eu^{3+}$ and magnetic Fe_3O_4 NPs are encapsulated simultaneously in the polymer nanospheres.

Figure 3 shows the luminescence spectra of NIP and MIP nanocomposites before and after removing the template

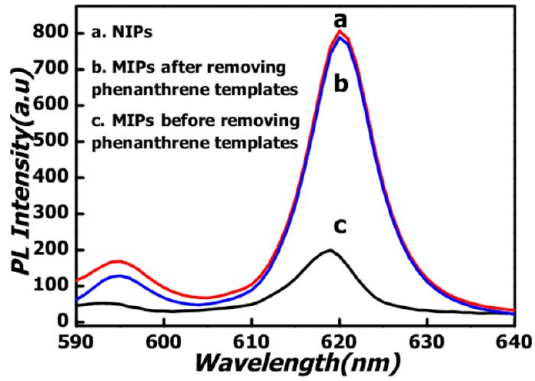

Figure 3. Luminescence spectra of the (a) NIP (200 μg) and MIP (200 μg) nanocomposites (c) before and (b) after removing the templates (phenanthrene) from the recognition cavities in MIPs. $\lambda_{em}/\lambda_{ex}$ = 620 nm/254 nm.

(phenanthrene) by elution. Compared to the luminescence of NIPs (Figure 3a), the red luminescence of MIPs was dramatically quenched by the embedded phenanthrene (Figure 3c). However, this quenched luminescence was almost completely recovered (Figure 3b) after the removal of templates by washing twice with acetone. The easy removal of the template by simple washing can be attributed to the relatively weak $\pi-\pi$ stacking and hydrophobic interactions between the polymer, hydrophobic NPs and phenanthrene. As a result, only a very small amount of solvent is needed, which gives both environmental and cost benefits.

The multifunctional MIP nanocomposite solution emits strong naked-eye-visible red luminescence under excitation at 254 nm. However, this strong luminescence is markedly quenched by PAHs. As shown in Figure 4, both the excitation (from Figure 4c to 4d) and luminescence (from Figure 4e to 4f) intensity of the as-prepared MIPs decreased on addition of phenanthrene (5.0 μg/mL), but the peak position in the spectra did not undergo any significant shift. To elucidate the luminescence quenching mechanism, UV−vis absorption spectra of anthracene, phenanthrene, pyrene, and perylene (5.0 μg/mL) were recorded (see Figure S1 in the Supporting Information). Comparison with the absorption spectrum of MIP nanocomposites in the absence of phenanthrene (Figure 4a) shows that the addition of phenanthrene (5.0 μg/mL) into the solution of MIPs results in a new UV−vis absorption band at 250 nm (Figure 4b) that partially overlaps with the excitation

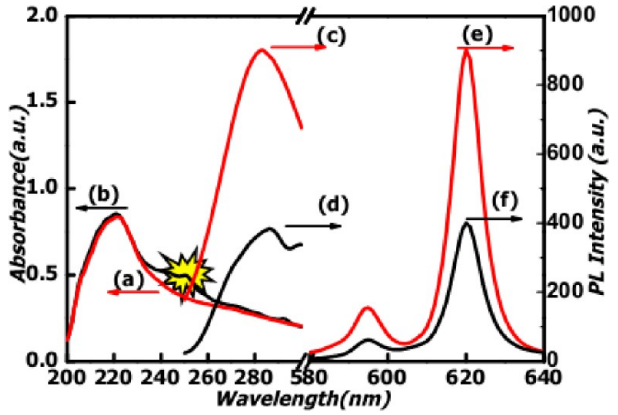

Figure 4. (a, b) UV–vis absorption, (c, d) excitation, and (e, f) emission spectra of the MIP nanocomposite solution (200 μg) before (red) and after (black) adding 5 μg/mL of phenanthrene. The solution was incubated at 25 °C and then separated using a magnet before luminescence detection.

spectrum (Figure 4c) of MIPs. The absorption peak resulting from the excitation of phenanthrene means that it acts as an energy acceptor and results in luminescence quenching of the fluorophores (which act as an energy donor).[37] We should mention that although the maximum excitation of the MIP nanocomposites is located at 280 nm, in order to avoid the interference of frequency-doubling scattering (560 nm) on the luminescence, 254 nm was chosen as the excitation wavelength in this work.

To understand the kinetics of the luminescence quenching, the time-dependent luminescence evolution upon addition of phenanthrene (5.0 μg/mL) was monitored at 25 °C (Figure 5).

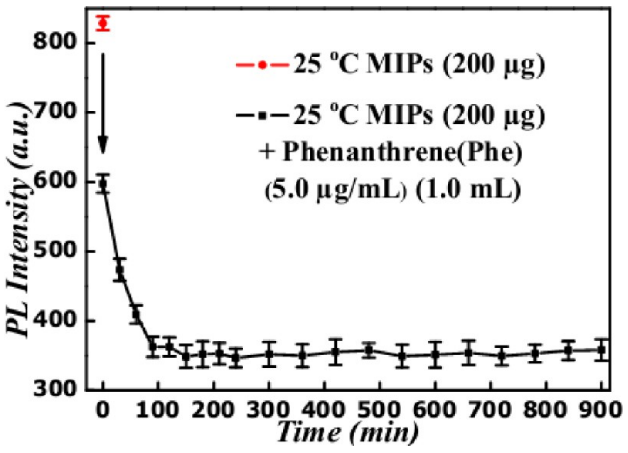

Figure 5. Time-dependent luminescence evolution upon addition of phenanthrene (5.0 μg/mL) to the MIP nanocomposites (200 μg). The solution was incubated at 25 °C and then separated using a magnet before luminescence detection.

The red luminescence showed an immediate marked quenching after addition of phenanthrene, decreased more slowly to a minimum after 90 min and then remained essentially unchanged (for at least 900 min), showing that the performance as a sensor for phenanthrene is quite stable. The initial steep decrease in luminescence results from the absorption of excitation energy by phenanthrene. The subsequent slower quenching can be attributed to energy transfer from the excited state of the luminescent NPs to phenanthrene incorporated into the recognition site in the MIP nanocomposites.[38] Moreover, as the temperature was increased from 45 to 65 to 85 °C (Figure 6), the minimum luminescence intensity was

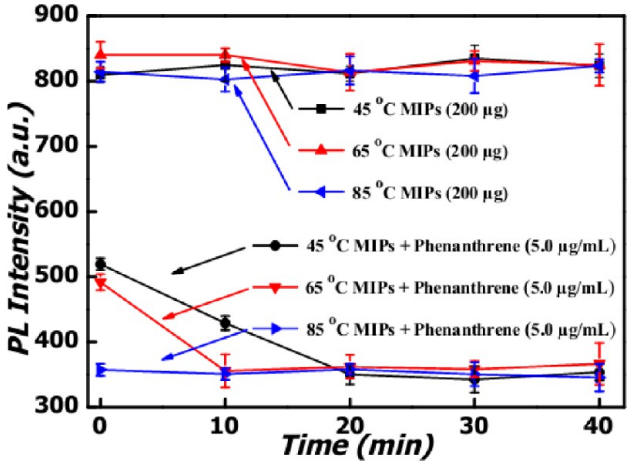

Figure 6. Influence of incubation time on the luminescence quenching reaction between the MIP nanocomposites (200 μg) and Phe (5.0 μg/mL) solution at different temperatures: 45 °C (black), 65 °C (red), and 85 °C (blue). The nanocomposites were collected using a magnet and redispersed before luminescence detection at room temperature (25 °C).

obtained after 20, 10, and 1 min, respectively, showing that increasing incubation temperature speeds up the rate of luminescence quenching. It should be mentioned that although the incubation was conducted at different temperatures, the luminescence detection was carried out after taking 1 mL of the incubated mixture solution and cooling to room temperature (25 °C). In other words, the incubation temperature has no effect on the final luminescence of the mixture, but it does have a great influence on the adsorption kinetics of phenanthrene in the MIP nanocomposites. In order to simplify the analysis process, the incubation was conducted at room temperature in the following tests. Figure 7 shows the luminescence spectra when different concentrations of phenanthrene were added to the nanocomposite colloidal solution. After incubation for 90 min at room temperature, the luminescence of MIPs was gradually quenched, with a corresponding color change from brilliant red to dark under a 254 nm UV lamp (inset in Figure 7).

To evaluate the specific recognition ability of the template sites in the MIP nanocomposites, the luminescence intensity of the nanocomposite solution was measured in the presence of different amounts of phenanthrene or other PAHs such as anthracene, pyrene or perylene. Unfortunately, as shown in Figure 8a, all the PAHs could quench the luminescence of the MIP nanocomposites due to their similar absorption bands (254 nm) (see Figure S1 in the Supporting Information), so that no selectivity for phenanthrene can be achieved. Therefore the MIP nanocomposites were pulled to one side of the vial by means of an external magnet and the supernatant was discarded. In the case of phenanthrene, as shown in Figure 8b, the luminescence of the MIP nanocomposites after magnetic separation decreased monotonically with increasing phenanthrene concentration in the original solution. More importantly, a good linear relationship between the relative emission intensity (I) of the colloidal solution of MIPs and the phenanthrene concentration (C, μg/mL) in the range 0.0–6.0

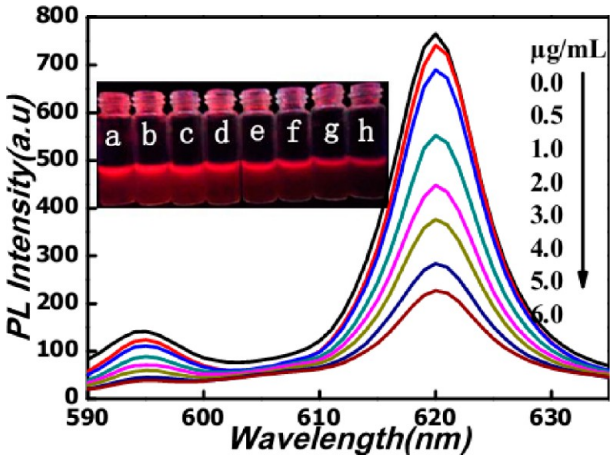

Figure 7. Variation in the luminescence of MIP nanocomposite solution (200 μg) with increasing phenanthrene concentration in the range 0.0–6.0 μg/mL. Inset: Luminescence of MIP nanocomposites after addition of different concentrations of phenanthrene: (a–h) 0.0, 0.5, 1.0, 2.0, 3.0, 4.0, 5.0, and 6.0 μg/mL. The solution was incubated at 25 °C for 90 min and then separated using a magnet before luminescence detection. These luminescence photos were obtained by discarding the supernatant after magnetic separation, and then dispersing the MIP nanocomposites in ethanol.

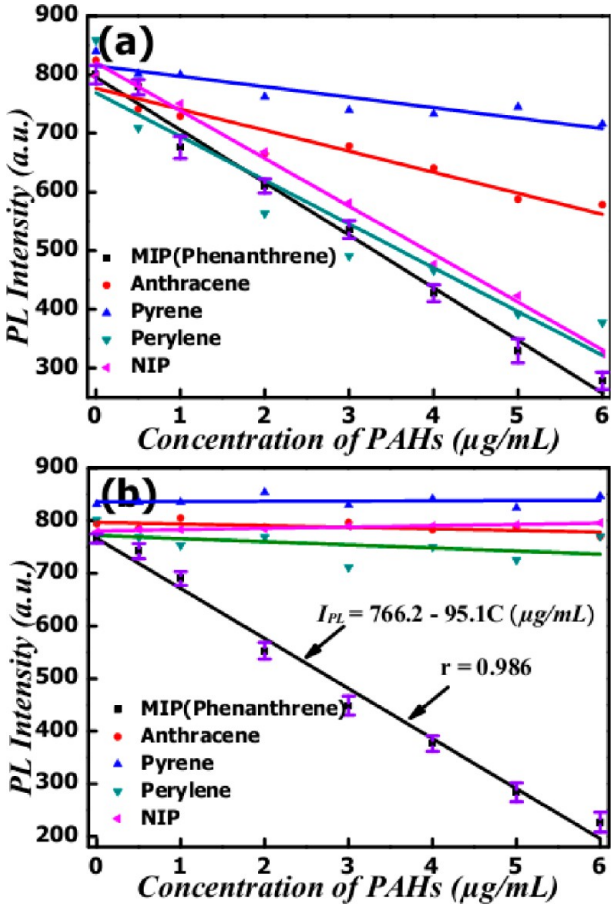

Figure 8. Calibration plots for phenanthrene and other PAHs (a) before and (b) after magnetic separation.

μg/mL was obtained (I = 766.2–95.1C, r = 0.986). The limit of detection (LOD = 3σ/K) for the target phenanthrene was calculated to be 3.64 ng/mL. In contrast, after magnetic separation of MIPs from solutions containing anthracene, pyrene, or perylene, no obvious luminescence quenching was observed, showing that the MIPs had excellent selectivity for the detection of phenanthrene. This is because anthracene, pyrene and perylene are not recognized by the phenanthrene-imprinted MIP nanocomposites and remain in the supernatant after magnetic separation. As a control, when phenanthrene solutions were analyzed using NIP nanocomposites without a magnetic separation step, the luminescence intensity gradually decreased with increasing phenanthrene concentration, whereas after magnetic separation, the phenanthrene had no influence on the luminescence of NIPs. This confirms that, as expected, the nanocomposites can recognize phenanthrene only if they have been imprinted with this molecule as a template.

The fact that anthracene, which has a very similar structure to phenanthrene (see the inset of Figure S1 in the Supporting Information), cannot be incorporated into the recognition site in the phenanthrene-templated MIPs and thus has no influence on the red emission of the nanocomposites after magnetic separation is an indication of the excellent selectivity of these materials. This selectivity is further confirmed by the photos of the MIP nanocomposite in the presence of different amount of anthracene shown in Figure 9. In daylight (Figure 9a) the colloidal solution of MIPs is milky white, and adding different concentrations of anthracene has no influence on the color of the colloidal solution. After a magnet was placed next to the vial, the MIP nanocomposites were drawn to the side wall of

Figure 9. Luminescence photos of the MIP nanocomposites (200 μg) (a, c) in daylight and (b, d) under 254 nm UV light (a, b) before and (c, d) after magnetic separation. Concentration of anthracene (a–h): 0.0, 0.5, 1.0, 2.0, 3.0, 4.0, 5.0, and 6.0 μg/mL.

dx.doi.org/10.1021/am4020605 | ACS Appl. Mater. Interfaces 2013, 5, 10502–10509

the vial leaving a colorless supernatant (Figure 9c), confirming the efficacy of magnetic separation. If the colloidal solution was irradiated by UV light (254 nm), the strong red luminescence was dramatically quenched in the presence of anthracene (Figure 9b). However, after magnetic separation, discarding the supernatant, and then redispersing the MIP nanocomposites in ethanol, the red luminescence was not quenched (Figure 9d). These results show that the combination of MIP nanocomposites and magnetic separation can offer good selectivity for the detection of target analytes.

To assess the wider applicability of our approach, we also fabricated MIP nanocomposites using pyrene instead of phenanthrene as the template. As shown in Figure 10a, all

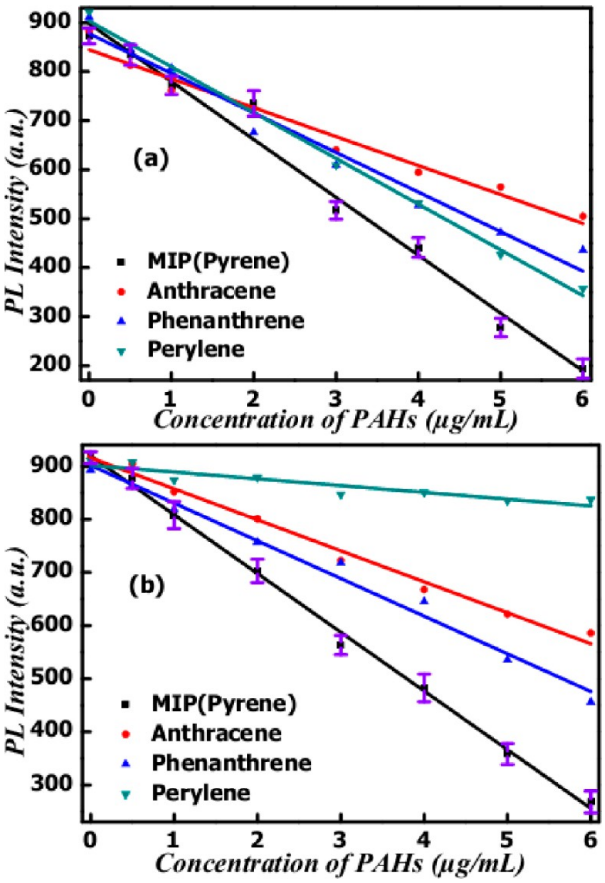

Figure 10. Variation in the luminescence of pyrene-templated MIPs (200 μg) in the presence of different concentrations of pyrene and other PAHs (a) before and (b) after magnetic separation.

the analytes—pyrene, anthracene, phenanthrene, and perylene—dramatically quench the red luminescence of the nanocomposites before magnetic separation. After magnetic separation (Figure 10b), the luminescence is still quenched in the presence of pyrene, as expected. However, the luminescence is also quenched in the presence of anthracene and phenanthrene as well, and only perylene gives no quenching of the luminescence. This disappointing selectivity can be understood by comparing the molecular structures of the PAHs (shown in the inset of Figure S1 in the Supporting Information), Both anthracene and phenanthrene have a similar chemical structure to pyrene, but are smaller molecules, which allows them to enter the specific recognition cavities of the pyrene-templated MIPs. However perylene has a larger molecular structure than pyrene and cannot access the pyrene-templated recognition sites. This highlights that our method should be applicable for the detection of different PAHs with satisfactory selectivity as long as the templates are carefully chosen.

To investigate the recognition and adsorption ability of the phenanthrene-templated MIP nanocomposites, we carried out thermodynamic binding experiments. Figure 11a shows the

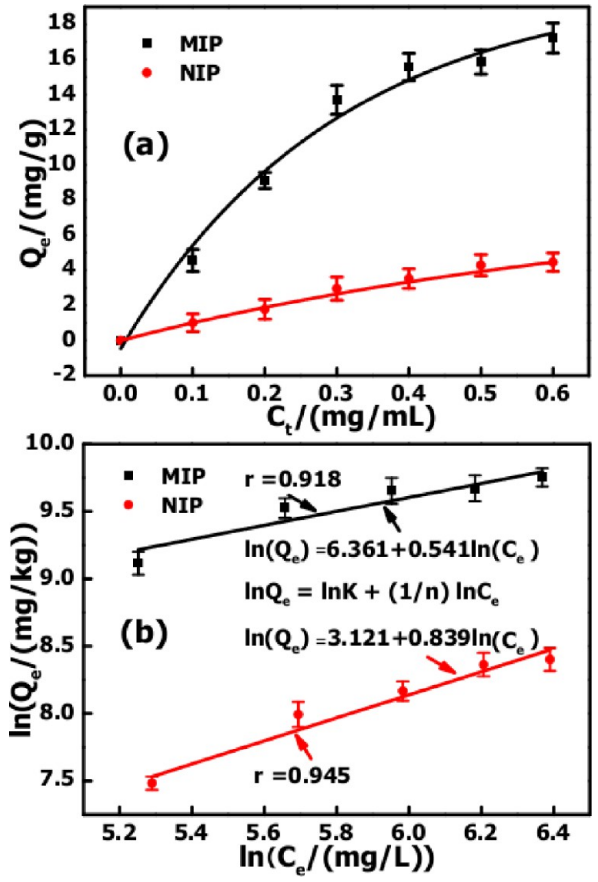

Figure 11. (a) Equilibrium adsorption isotherms and (b) Freundlich fit for the binding of phenanthrene by MIP nanocomposites (black line) and NIP nanocomposites (red line). C_t and C_e are the concentrations of initial and free phenanthrene, respectively. Nanocomposites, 8 mg (MIPs) and 9 mg (NIPs); volume, 2.0 mL.

binding isotherms of phenanthrene on the MIPs and NIPs. The equilibrium adsorption amount (Q_e) can be calculated according to eq 1

$$Q_e = (C_t - C_e)Vm^{-1} \quad (1)$$

,where Q_e is the amount of bound phenanthrene (mg/g) after the adsorption reaches equilibrium, C_t and C_e are the initial and equilibrium concentration of phenanthrene (mg/mL), respectively, V is the volume of the mixture (mL), and m represents the amount of MIPs or NIPs (g). The adsorption capacity of phenanthrene (Q_e) increases rapidly with increasing initial concentration (C_t) of phenanthrene (Figure 11a). When C_t is higher than 4.0 mg/mL, the adsorption ability of MIPs becomes saturated. The amount of phenanthrene adsorbed in the nanocomposites is 15.57 mg/g. NIPs show the same trend as that for MIPs, but have a much lower saturated adsorption loading (3.52 mg/g). This corresponds to an imprinting factor

dx.doi.org/10.1021/am4020605 | ACS Appl. Mater. Interfaces 2013, 5, 10502−10509

(M_{MIP}/M_{NIP}) of 4.42, which highlights the efficacy of molecular imprinting.

As shown in Figure 11b, the experimental equilibrium adsorption data for phenanthrene on MIP nanocomposites can be fitted to the Freundlich equation[32,39] by linear regression analysis with eq 2

$$\ln Q_e = \ln K + (1/n)\ln C_e \quad (2)$$

,where K and n are the constants of the Freundlich equation. The value of $(1/n)$ can be calculated from the slope of the isotherm curve and can be utilized to evaluate the adsorption affinity of the MIPs.[40] Lower $(1/n)$ values correspond to higher adsorption affinity and vice versa. The values of $1/n$ for MIPs (0.541) and NIPs (0.839) confirm that the phenanthrene-templated MIP nanocomposites have higher affinity for phenanthrene.

In order to evaluate the stability of our nanocomposite sensor, pure phenanthrene and phenanthrene-containing mixtures of PAHs were incubated with the phenanthrene-templated MIP nanocomposites at 25 °C for 90 min before magnetic separation and luminescence detection. As shown in Table 1, satisfactory recoveries ranging from 96.87 to 100.4%

Table 1. Results of Phenanthrene Assay of Mixed Samples of PAHs[a]

	concentration (μg/mL)		
sample	added	found Phe (mean, measurement number n = 4)	recovery (%)
Phe	5.0	5.02 ± 0.02	100.4 ± 0.30
Phe/Ant	5.0/2.0	4.84 ± 0.03	96.87 ± 0.61
Phe/Pyr	5.0/2.0	5.02 ± 0.06	100.4 ± 1.16
Phe/Per	5.0/2.0	4.97 ± 0.07	99.47 ± 1.32
Phe/Ant/Pyr/Per	5.0/2.0/2.0/2.0	4.95 ± 0.04	98.95 ± 0.78

[a]Phe = phenanthrene, Ant = anthracene, Pyr = pyrene, and Per = perylene.

were obtained. The results further confirm that the MIP nanocomposites possess excellent molecular recognition ability and constitute a very simple assay for the selective determination of phenanthrene in mixtures of PAHs.

To assess the practicality of our method for use with real samples, the as-prepared MIP nanocomposites were used to pre-concentrate and monitor trace PAHs in commercial milk samples. Up to now, the main problem with the detection of trace PAHs in milk is their very low concentration and the complexity of the samples. As a consequence, the preconcentration and purification of target analytes is necessary to obtain good selectivity and high sensitivity. Therefore, the development of a nanocomposite MIP-based method for selective PAH analysis in complex samples such as milk is highly desirable. As shown in Table 2, when different milk samples were spiked with 5.0 μg/mL of phenanthrene and analyzed after magnetic separation and redispersion in ethanol, the recoveries of the sensor ranged from 97.11 to 101.9%, which is an indicator of its good accuracy and practicability for use with real samples.

CONCLUSIONS

By combining magnetic separation and specific molecular recognition, multifunctional molecularly imprinted polymer (MIP) nanocomposites (Fe_3O_4/$LaVO_4$:Eu^{3+}@MIPs) have been successfully fabricated and employed for the highly selective and sensitive luminescence monitoring of polycyclic aromatic persistent organic pollutants (POPs) in mixtures. It is worth mentioning that our method is especially suitable for the preparation of MIPs with the majority of POPs, which have no active functional groups to form hydrogen bonds or covalent bonds with the monomer during the formation of MIPs. The resulting MIP nanocomposites have great potential for the preconcentration and selective detection of trace POPs in complex samples since they offer the advantages of simplicity, high sensitivity, good selectivity, low cost, and visual detection. This work paves the way to develop multifunctional magnetic–luminescent MIP nanosensors, which will find many applications in the fields of environmental, chemical, and biomedical sensing.

Table 2. Results of Phenanthrene Detection in Milk Samples

	phenanthrene concentration (μg/mL)		
sample	added	found (mean, measurement number n = 4)	recovery (%)
milk 1 (Mengniu)	5.0	4.96 ± 0.04	99.32 ± 0.88
milk 2 (Yili)	5.0	5.09 ± 0.02	101.9 ± 0.42
milk 3 (Sanyuan)	5.0	4.86 ± 0.03	97.11 ± 0.58

ASSOCIATED CONTENT

Supporting Information

Chemical structures and UV–vis absorption spectra of anthracene, phenanthrene, pyrene, and perylene (5.0 μg/mL). This material is available free of charge via the Internet at http://pubs.acs.org.

AUTHOR INFORMATION

Corresponding Author

*E-mail: lywang@mail.buct.edu.cn. Tel: (086) 010-64427869. Fax: (086) 010-64427869.

Notes

The authors declare no competing financial interest.

ACKNOWLEDGMENTS

This work was supported in part by the State Key Project of Fundamental Research of China (2011CB932403), the National Natural Science Foundation of China (21275015, 21075009), and the Program for New Century Excellent Talents in University of China (NCET-10-0213), and the Scientific Research Foundation for the Returned Overseas Chinese Scholars, State Education Ministry. We thank Prof. David G. Evans for his careful polish on this manuscript.

REFERENCES

(1) Bente, M.; Sklorz, M.; Streibel, T.; Zimmermann, R. *Anal. Chem.* **2009**, *81*, 2525–2536.
(2) Emmenegger, C.; Kalberer, M.; Samburova, V.; Zenobi, R. *Analyst* **2004**, *129*, 416–420.
(3) Barnes, J. C.; Juricek, M.; Strutt, N. L.; Frasconi, M.; Sampath, S.; Giesener, M. A.; McGrier, P. L.; Bruns, C. J.; Stern, C. L.; Sarjeant, A. A.; Stoddart, J. F. *J. Am. Chem. Soc.* **2013**, *135*, 183–192.
(4) Conney, A. H. *Cancer Res.* **1982**, *42*, 4875–4917.
(5) Del Carlo, M.; Di Marcello, M.; Giuliani, M.; Sergi, M.; Pepe, A.; Compagnone, D. *Biosens. Bioelectron.* **2012**, *31*, 270–276.
(6) Nizzetto, L.; Macleod, M.; Borga, K.; Cabrerizo, A.; Dachs, J.; Di Guardo, A.; Ghirardello, D.; Hansen, K. M.; Jarvis, A.; Lindroth, A.;

Ludwig, B.; Monteith, D.; Perlinger, J. A.; Scheringer, M.; Schwendenmann, L.; Semple, K. T.; Wick, L. Y.; Zhang, G.; Jones, K. C. *Environ. Sci. Technol.* **2010**, *44*, 6526−6531.
(7) Niu, H. Y.; Wang, Y. X.; Zhang, X. L.; Meng, Z. F.; Cai, Y. Q. *ACS Appl. Mater. Interfaces* **2012**, *4*, 286−295.
(8) Segro, S. S.; Triplett, J.; Malik, A. *Anal. Chem.* **2010**, *82*, 4107−4113.
(9) Bai, D. S.; Li, J. L.; Chen, S. B.; Chen, B. H. *Environ. Sci. Technol.* **2001**, *35*, 3936−3940.
(10) Zhu, Y.; Morisato, K.; Li, W. Y.; Kanamori, K.; Nakanishi, K. *ACS Appl. Mater. Interfaces* **2013**, *5*, 2118−2125.
(11) Pandey, S. K.; Kim, K. H.; Brown, R. J. C. *TrAC—Trends Anal. Chem.* **2011**, *30*, 1716−1739.
(12) Zeigler, C. D.; Robbat, A. *Environ. Sci. Technol.* **2012**, *46*, 3935−3942.
(13) Zeigler, C.; Wilton, N.; Robbat, A. *Anal. Chem.* **2012**, *84*, 2245−2252.
(14) Benhabib, M.; Chiesl, T. N.; Stockton, A. M.; Scherer, J. R.; Mathies, R. A. *Anal. Chem.* **2010**, *82*, 2372−2379.
(15) Guerrini, L.; Garcia-Ramos, J. V.; Domingo, C.; Sanchez-Cortes, S. *Anal. Chem.* **2009**, *81*, 953−960.
(16) Alvarez-Puebla, R. A.; Dos Santos, D. S.; Aroca, R. F. *Analyst* **2007**, *132*, 1210−1214.
(17) Ma, Y. R.; Zhang, X. L.; Zeng, T.; Cao, D.; Zhou, Z.; Li, W. H.; Niu, H. Y.; Cai, Y. Q. *ACS Appl. Mater. Interfaces* **2013**, *5*, 1024−1030.
(18) Gao, D. M.; Zhang, Z. P.; Wu, M. H.; Xie, C. G.; Guan, G. J.; Wang, D. P. *J. Am. Chem. Soc.* **2007**, *129*, 7859−7866.
(19) Haupt, K.; Mosbach, K. *Chem. Rev.* **2000**, *100*, 2495−2502.
(20) Banerjee, S.; Konig, B. *J. Am. Chem. Soc.* **2013**, *135*, 2967−2970.
(21) Sellergren, B.; Lepisto, M.; Mosbach, K. *J. Am. Chem. Soc.* **1998**, *110*, 5853−5860.
(22) Hong, C. C.; Chang, P. H.; Lin, C. C.; Hong, C. L. *Biosens. Bioelectron.* **2010**, *25*, 2058−2064.
(23) Huang, Y. P.; Zheng, C.; Liu, Z. S. *Curr. Org. Chem.* **2011**, *15*, 1863−1870.
(24) Chen, L. X.; Xu, S. F.; Li, J. H. *Chem. Soc. Rev.* **2011**, *40*, 2922−2942.
(25) Li, H. F.; Xie, C. G.; Li, S. Q.; Xu, K. *Colloids Surf., B* **2012**, *89*, 175−181.
(26) Xie, C. G.; Li, H. F.; Li, S. Q.; Gao, S. *Microchim. Acta* **2011**, *174*, 311−320.
(27) Xie, C. G.; Li, H. F.; Li, S. Q.; Wu, J.; Zhang, Z. P. *Anal. Chem.* **2010**, *82*, 241−249.
(28) Jones, K. C.; de Voogt, P. *Environ. Pollut.* **1999**, *100*, 209−221.
(29) Liu, J. L.; Liu, Y.; Liu, Q.; Li, C. Y.; Sun, L. N.; Li, F. Y. *J. Am. Chem. Soc.* **2011**, *133*, 15276−15279.
(30) Tu, N. N.; Wang, L. Y. *Chem. Commun.* **2013**, *49*, 6319−6321.
(31) Ma, Y. X.; Li, H.; Peng, S.; Wang, L. Y. *Anal. Chem.* **2012**, *84*, 8415−8421.
(32) Zhao, Y. Y.; Ma, Y. X.; Li, H.; Wang, L. Y. *Anal. Chem.* **2012**, *84*, 5447−5447.
(33) Ma, Y. X.; Li, H.; Wang, L. Y. *J. Mater. Chem.* **2012**, *22*, 18761−18767.
(34) Liang, X.; Wang, X.; Zhuang, J.; Chen, Y. T.; Wang, D. S.; Li, Y. D. *Adv. Funct. Mater.* **2006**, *16*, 1805−1813.
(35) Liu, J. F.; Li, Y. D. *Adv. Mater.* **2007**, *19*, 1118−1122.
(36) Zhu, Y. Y.; Zhao, Y. Y.; Ma, Y. X.; Deng, M. L.; Wang, L. Y. *Luminescence* **2012**, *27*, 74−79.
(37) Yuan, P.; Walt, D. R. *Anal. Chem.* **1987**, *29*, 2391−2394.
(38) Gao, D. M.; Wang, Z. Y.; Liu, B. H.; Ni, L.; Wu, M. H.; Zhang, Z. P. *Anal. Chem.* **2008**, *80*, 8545−8553.
(39) Kumar, K. V.; de Castro, M. M.; Martinez-Escandell, M.; Molina-Sabio, M.; Rodriguez-Reinoso, F. *J. Phys. Chem. C* **2010**, *114*, 13759−13765.
(40) Rampey, A. M.; Umpleby, R. J.; Rushton, G. T.; Iseman, J. C.; Shah, R. N.; Shimizu, K. D. *Anal. Chem.* **2004**, *76*, 1123−1133.